The 2D Coulomb gas on a 1D lattice

1999 J. Phys. A: Math. Gen. 32 1131

(http://iopscience.iop.org/0305-4470/32/7/005)

J. Phys. A: Math. Gen. **32** (1999) 1131–1146. Printed in the UK PII: S0305-4470(99)99790-1

The 2D Coulomb gas on a 1D lattice

Onuttom Narayan† and B Sriram Shastry‡

† Physics Department, University of California, Santa Cruz, CA 95064, USA
‡ Physics Department, Indian Institute of Science, Bangalore 560012, India

Received 30 November 1998

Abstract. The statistical mechanics of a two-dimensional Coulomb gas confined to one dimension is studied, wherein hard core particles move on a ring. Exact self-duality is shown for a version of the sine-Gordon model arising in this context, thereby locating the transition temperature exactly. We present asymptotically exact results for the correlations in the model and characterize the low- and high-temperature phases. Numerical simulations provide support to these renormalization group calculations. Connections with other interesting problems, such as the quantum Brownian motion of a particle in a periodic potential and impurity problems, are pointed out.

1. Introduction

The physics of the inverse-squared exchange Heisenberg model, the so-called Haldane Shastry model [1, 2] has been a field of considerable activity recently. Here one considers a spin-$\frac{1}{2}$ Heisenberg antiferromagnet in one dimension on a ring of L sites with an exchange Hamiltonian

$$H = J \sum_{i<j} \frac{\phi^2}{\sin(\phi(x_i - x_j))^2} \vec{S}_i \cdot \vec{S}_j \tag{1}$$

with x_j as integers denoting lattice points and $\phi = \pi/L$. The ground state of the model of equation (1) in a sector with N spin reversals (relative to the ferromagnet) located at $\{\ldots x_j \ldots\}$ is given by

$$\psi(x_1, x_2, \ldots, x_N) = (-1)^{\sum x_j} \prod_{i<j} \sin^{\beta/2}(\phi(x_j - x_i)) \tag{2}$$

with $\beta = 4$. The model is interesting from several points of view, such as the connection with Gutzwiller projection in strongly correlated systems, and from the intimate connection with the isotropic Heisenberg antiferromagnet, the Bethe chain. The spin–spin correlation function of the above wavefunction at $\beta = 4$ has the same decay exponent as the Bethe chain, namely unity. Further, at $\beta = 2$, the wavefunction is the ground state of the free Fermi gas, with either long-ranged hops or just nearest neighbour hops. The first case at $\beta = 2$ corresponds to dropping the zz part of equation (1), and the second to the anisotropic Heisenberg model: $H = \sum_i (S_i^x S_{i+1}^x + S_i^y S_{i+1}^y + \Delta S_i^z S_{i+1}^z)$ at $\Delta = 0$. Thus we find that $\beta = 4$ and 2 are in close correspondence with $\Delta = 1$ and 0, respectively. The Heisenberg model is well known [3] to have a transition to a massive Nèel ordered phase at $\Delta = 1$, and so one might suspect that the wavefunction in equation (2) could develop long-ranged order (LRO) as β increases from 4, perhaps even at $\beta = 4^+$, a possibility we shall investigate in this paper. It is obvious that Nèel order can also be viewed as crystalline order of hard core bosons, where the bosons correspond to the spin reversals of the Heisenberg system via the familiar lattice gas analogy. We will

0305-4470/99/071131+16$19.50

almost exclusively use this point of view below. Note that the density variables $\rho_i = (\frac{1}{2} - S_i^z)$ take values 0, 1 so that we can map density correlators to spins readily, with N the number of hard core particles restricted to $N \leqslant L/2$.

For the case of $\beta \neq 2, 4$ the wavefunctions do not represent either symmetric or antisymmetric functions, and are hard to interpret as physically allowed states for bosons/fermions, unless one imposes a rather non-analytic restriction of taking the modulus. For larger even integer values of $\beta = 6, 8 \ldots$ the wavefunction in equation (2) is an eigenstate of the anisotropic version of the Hamiltonian in equation (1), but only in restricted sectors of numbers of particles, for fillings up to $\frac{2}{\beta}$, since beyond this filling the states are no longer 'good functions' in the sense of [4], i.e. they have Fourier components that 'spill out' of the first Brillouin zone, requiring umklapp.

The evaluation of correlations in the above wavefunction reduces to those of a 2D Coulomb gas confined to a 1D ring, but with the positions of the particles discretized to a lattice. This is a far reaching distinction from the case where the charged particles are in the continuum, a case that is familiar from the well known results of Dyson, Mehta and Gaudin [5] for random matrices. In the latter case, the Coulomb gas does not crystallize in the sense of possessing LRO, although the density correlators are arbitrarily slowly decaying. In the lattice case one expects LRO, which is consistent with Nèel order.

The discrete Coulomb gas (DCG) has been subject to a few exact calculations. Gaudin [6] computed the normalization constant of the wavefunction and the grand partition function exactly at three values of $\beta = 1, 2, 4$. His isothermal calculation of the grand partition function at these values of the temperature gives the distribution of zeros in the thermodynamic limit as lying on segments of the unit circle. Mehta and Mehta [7] computed the density correlators exactly at these values of β. The calculations at $\beta = 2$ are not unexpected, since the model at $\beta = 2$ reduces to a free Fermi lattice-gas, but the other cases are highly non-trivial. Sutherland [8] has presented results at zero temperature for the allowed ground state patterns, that turn out to be quite complex for arbitrary rational fillings.

In this paper, we present some asymptotically exact results on this problem, using a combination of renormalization group (RG), and exact duality arguments on related models. We only consider simple rational fillings in this work with filling $f = \frac{N}{L} = \frac{1}{2}, \frac{1}{3}, \frac{1}{4} \ldots$ We find that for each such filling f there is a transition temperature $\beta_c = 2/f^2$ at which the LRO sets in. In section 2 of this paper, we show that the DCG is asymptotically equivalent to a sine-Gordon model that has recently been studied extensively in connection with several interesting problems. This is achieved through a series of approximations that lead to a phonon representation at high temperatures, and a kink representation at low temperatures. Correlation functions are discussed in both representations. In section 3, the analogues of the phonon and kink representations are constructed for a model asymptotically equivalent to the DCG, and an exact duality connecting the two pictures is obtained. The duality found by us is closely related to that found by Kjaer and Hilhorst [9], who studied a discrete height problem—a roughening model, where the heights interact via a $1/r^2$ interaction. Our sine-Gordon model reduces to this model on integrating out the Gaussian displacements. Section 4 presents numerical results that confirm the results of the previous sections and the difficulties involved in extracting true exponents are highlighted. Connections to related models and other general issues are discussed in section 5.

2. Phonon and kink representations

In order to understand the spin correlations for these wavefunctions, it is convenient to convert the problem into one in classical statistical mechanics. For a ring with $N = fL$ spins, if $\psi(x_1, x_2 \dots x_N)$ is the amplitude for the down spins located at $x_1, x_2 \dots x_N$, then $|\psi(x_1, x_2 \dots x_N)|^2$ is the corresponding probability. By rotational symmetry, the spin–spin correlation function $\langle \boldsymbol{S}(x) \cdot \boldsymbol{S}(y) \rangle$ is equal to $3S_z(x)S_z(y)$. This can be calculated from $|\psi|^2$, without any knowledge of the phase of ψ. (This is not possible in general for higher-order correlations, where one cannot always get rid of S_+ and S_- operators by symmetry arguments. In this paper, we shall only consider two-point correlations.)

If we express $|\psi(x_1, x_2 \dots x_N)|^2$ as $\exp[\ln |\psi|^2]$, we can view $-\ln |\psi|^2$ as the energy of a classical system of N particles (distributed over $L = N/f$ sites), and $|\psi|^2$ as the statistical weight assigned in thermal equilibrium to a particle configuration. For the wavefunctions we consider here, $-\ln |\psi|^2$ has the form

$$-\ln |\psi(x_1, x_2 \dots x_N)|^2 = -\frac{\beta}{2} \sum_{i<j} \ln[\phi^{-2} \sin^2 \phi(x_i - x_j)] + \text{const.} \tag{3}$$

The additive constant at the end of the right-hand side is necessary in order to ensure that the wavefunction is normalized; however, in the statistical mechanics picture, it only gives rise to an overall proportionality factor in the partition function, and can be ignored. The $1/\phi^2$ inside the argument of the logarithm has been pulled out from the additive constant so that the $L \to \infty$ limit exists.

Equation (3) describes a collection of particles with pairwise interactions. Every particle repels every other particle logarithmically. The argument of the logarithm is effectively (the square of) the straight line (or chord) distance between two points, x_i and x_j, on the ring. Thus the system consists of a charged gas with 2D Coulomb interactions, but with the particles confined to a (1D) ring lattice. The prefactor β has a natural interpretation of the inverse temperature.

In its ground state, the system has one particle on every $1/f$th site, at least for simple fractions f that we consider here (say $\frac{1}{2}$, $\frac{1}{3}$ etc). As the temperature is lowered, i.e. β is raised, there is the prospect of the system crystallizing into a LRO state. As we shall see in this paper, this indeed happens at $\beta = 2/f^2$, and is the result of a combination of two factors. Firstly, although one normally expects short-range order in a 1D system, the long-ranged logarithmic interactions convert this to quasi LRO even at high temperatures. Secondly, the restriction that particles can only be placed on lattice sites crystallizes the system at low temperatures.

There are two complementary approximations that one can make on the ring-lattice Coulomb gas, one appropriate for high temperatures and one for low temperatures. Both these approximations yield a 1D long-ranged sine-Gordon model, but with different parameters, reflecting the well known duality of this model. This duality is usually derived for a continuum sine-Gordon model [10], but there are slight differences for the lattice version, as we shall now see.

2.1. Phonon representation

At high temperatures, there are large fluctuations in the separation between neighbouring particles. It is reasonable to expect that, in this regime, the underlying lattice constraint might not be very important. Accordingly, in equation (3), we express $x_i = \frac{1}{f}(i + u_i)$, where u_i/f is the deviation from an ideal crystalline state. The hard lattice constraint is replaced with a

periodic potential, to obtain

$$\beta H[\{u\}] = -\frac{\beta}{2}\sum_{i<j}\ln\left[\frac{L^2}{\pi^2}\sin^2\frac{\pi(i+u_i-j-u_j)}{fL}\right]+\sum_i V(u_i). \tag{4}$$

The u_i are now continuous variables, and the potential V favours locating the particles at lattice sites. As an example consider $V(u_i) = -|\text{const}|\cos(2\pi x_i)$ which reduces to $-|\text{const}|\cos(2\pi u_i/f)$, leading to the sine-Gordon theory considered below. More formally, the hard lattice constraint can be expressed in terms of a singular periodic potential V: $V(u) = \ln[\sum_n \exp(2\pi n i u/f)]$. We shall instead consider the general class of potentials with periodicity f, and later exploit the universality under the RG. Expanding the first term on the right-hand side of equation (4), to second order in u we have

$$\beta H[\{u\}] = \frac{\beta}{4}\frac{\pi^2}{N^2}\sum_{i<j}\frac{(u_i-u_j)^2}{\sin^2[\pi(i-j)/N]}+\sum_i V(u_i). \tag{5}$$

In Fourier space, expanding $u_j = \sum_q(\tilde{u}_q/\sqrt{N})\exp[\mathrm{i}jq]$, it can be shown† that this is equivalent to

$$\beta H[\{u\}] = \frac{\beta}{2}\sum_q(\pi|q| - q^2/2)\tilde{u}_q\tilde{u}_{-q}+\sum_i V(u_i). \tag{6}$$

The sum over q ranges from $-\pi$ to π. Compared with the $\pi|q|$ term, the q^2 is irrelevant in the RG sense, and can be ignored in calculating long wavelength properties. Higher-order terms in the expansion of equation (4) in powers of u are similarly unimportant, as we see later.

2.2. Coulomb gas

We now cast the problem of computing the partition function for equation (6) in the form of another Coulomb gas, but with a variable number of charge pairs, controlled by a chemical potential. Writing a general expansion $\exp(-V(u_j)) = \sum_{m_j} c_{m_j}\exp(2\pi\mathrm{i}u_j m_j/f)$, consistent with the periodicity $u \to u + f$ we consider the partition function

$$Z = \int[\mathrm{d}u]\exp\left[-\sum_q G(q)\tilde{u}_q\tilde{u}_{-q}\right]\prod_j\left(\sum_{m_j} c_{m_j}\mathrm{e}^{2\pi\mathrm{i}u_j m_j/f}\right) \tag{7}$$

where the u_j are continuous variables, and $G(q)$ is some function of q. (Corresponding to equation (6), one would have $G(q) = (\beta/2)(\pi|q| - q^2/2)$.) This is equivalent to

$$Z = \sum_{m_1}\sum_{m_2}\cdots\int[\mathrm{d}u]\exp\left[-\sum_q G(q)\tilde{u}_q\tilde{u}_{-q}\right]\left(\prod_j c_{m_j}\right)\mathrm{e}^{2\pi\mathrm{i}/f\sum_j u_j m_j}. \tag{8}$$

If $G(q=0) = 0$, the only terms in this sum that are not zero are those for which $\sum_j m_j = 0$. Integrating out the u, we have

$$Z \propto \sum_{m_1}\sum_{m_2}\cdots\delta_{\sum m_j,0}\left(\prod_j c_{m_j}\right)\exp\left[-\pi^2/f^2\sum_q(\tilde{m}_q\tilde{m}_{-q})/G(q)\right]. \tag{9}$$

This is the partition function for a charged gas. (If we restrict c_m to be non-zero only for $m = \pm 1$ or 0, we have a dilute gas of unit positive and negative charges.) Using the fact that $\sum_j m_j = 0$, the exponent in the exponential is equal to

$$\frac{2\pi^2}{Lf^2}\sum_{i<j}m_i m_j\sum_q\frac{1-\cos q(i-j)}{G(q)} = \frac{\pi}{f^2}\sum_{i<j}m_i m_j\int\mathrm{d}q\,\frac{1-\cos q(i-j)}{G(q)} \tag{10}$$

† We use $(\frac{\pi}{N})^2\sum_{n=1}^{N-1}\mathrm{cosec}^2(\frac{n\pi}{N})\exp(\mathrm{i}kn) = -|k|\pi + \frac{1}{2}k^2 + \frac{\pi^2}{3}(1-\frac{1}{N^2})$ with $-\pi \leqslant k \leqslant \pi$.

where we have taken the $L \to \infty$ limit in the last step. For the case $G(q) = \frac{\pi\beta}{2}|q|$, i.e. the leading low-energy part of equation (6), we can evaluate the integral easily for large separation of the charges, and find the dilute Coulomb gas partition function:

$$Z_{k-\bar{k}} = \sum_{m_i=-\infty}^{\infty} \delta_{\Sigma m_i=0}\left(\prod_j c_{m_j}\right) \exp\left[-\beta_{eff}\left\{-\sum_{i<j} \log|i-j| m_i m_j - \mu_{eff}\sum m_i^2\right\}\right] \tag{11}$$

with $\beta_{eff} = \frac{4}{\beta f^2}$ and the 'chemical potential' $\mu_{eff} = -(\gamma + \log\pi)/2 = -0.860\,973$ with γ Euler's constant (0.577 216). The Coulomb interaction binds unlike charges, and repels like charges. The quadratic terms of $G(q)$ give rise to a sublogarithmic part in the interaction energy, but do not affect μ_{eff}. The object μ_{eff} is not really a chemical potential, since the relative weights assigned to different charges depends on the coefficients $\{c_m\}$. However, for large β_{eff}, where the partition function is dominated by $m_i = 0, \pm 1$, μ_{eff} may be viewed as the chemical potential associated with the (unit) positive and negative charges in the system, provided that $c_{\pm 1} = c_0$. Alternatively, μ_{eff} can be absorbed in a redefinition of the coefficients c_m, and is included when we start with general periodic potentials in equation (6).

2.3. Kink representation

In order to develop this representation, it is convenient to first rewrite equation (3) as

$$\beta H[\{\rho\}] = -\beta f^2 \sum_{\{i<j\}} m_i m_j \ln\left[\frac{L}{\pi}\left|\sin\frac{\pi(i-j)}{L}\right|\right] + \text{const.} \tag{12}$$

The variable m_i is $(1-f)/f$ if the site i is occupied, and -1 if the site is unoccupied. Compared with equation (3), this is equivalent to adding a background charge of $-f$ at every lattice site, and then reducing the unit of charge to f; although this changes the total energy (the additive constant in equation (12) is different from that in equation (3)), the energy difference between different configurations—and therefore their relative statistical weight—is unaltered.

At low temperatures, the system is in an almost perfect crystalline state, with one particle after every $1/f$ sites. There are long segments that are shifted by l sites with respect to a reference crystalline state, with $l = 0, 1, 2 \ldots (1/f - 1)$. (Shifting a segment by $1/f$ sites is equivalent to not shifting it at all.) There is an effective build-up of charge at the 'kinks' at the segment boundaries. At low temperatures, the dominant configurations have neighbouring segments with a relative shift ± 1 corresponding to a unit positive charge (a kink) or a unit negative charge (an antikink) at the segment boundary. Note that there is *no* alternation rule for the kinks here, unlike the case for a system where the ground state has ferromagnetic order rather than antiferromagnetic.

We now show that the energy of the system can be understood as an interaction of these charged kinks. As illustrated in figure 1, two neighbouring segments can be viewed

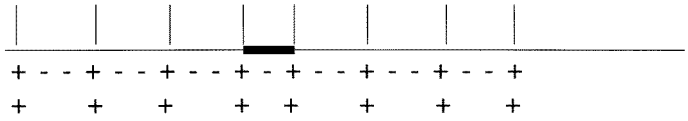

Figure 1. Typical lattice segment for $f = \frac{1}{3}$. Every positively charged site is doubly charged. The vertical lines denote the boundaries between adjacent quadrupoles, and lie on the midpoints of the positively charged sites. The thick section in the middle of the line segment is a kink, consisting of one positive charge at either end and only *one* negative charge inside. The total charge of the kink is thus +1.

as each consisting of a long string of quadrupoles, with a residual charge between them. Each quadrupole consists of $f-1$ negative charges terminated by a charge $+(f-1)/2$ at either end. The residual charge associated with the kink is ± 1; in figure 1, it is +1. Since the interaction energy between a quadrupole at i and a charge at j decays as $1/(i-j)^2$, the total interaction energy between *all* the quadrupoles in a segment and a kink not at its terminus decays as $1/l$ when the typical segment size is l. The interaction between the quadrupoles in non-adjacent segments can likewise be neglected. One is left with the interaction between the kinks. (The interaction between a kink and its adjacent segments, or two neighbouring segments separated by a kink, can be interpreted as a self-energy or chemical potential for the kink; as in the previous section, we need not keep track of this.) The final picture that emerges is equation (11), with m_i restricted to $0, \pm 1$ and β_{eff} replaced by βf^2.

2.4. Relationship between the representations

The kink–antikink gas, that we derived from equation (3) by a sequence of approximations, thus leads to a partition function that is essentially the *same* as obtained in the phonon representation, except that βf^2 is replaced by $4/\beta f^2$. This is not surprising, since the continuum 1D long-ranged sine-Gordon model has such a duality [10]. However, in the discrete version, when the strength of the potential $V(u_i)$ in equation (4) tends to infinity, corresponding to a lattice model, the fugacity of the kinks in the kink representation does not tend to zero. This is because u_i can jump from one integer to another when the discrete variable i is increased by unity, whereas discontinuities in $u(x)$ are not allowed in the continuum version.

For $\beta = 2/f^2$, the system is at its self-dual point. Of course, the duality that we have arrived at is only an approximate one. In particular, if one starts from equation (3) at the self-dual $\beta = 2/f^2$, and proceeds along the phonon and kink routes, the resultant chemical potentials and various sublogarithmic interaction terms are different. In section 3, we shall obtain an exact duality for a model using a restricted class of periodic potentials $V(u)$, and a phonon spectrum that is linear in $|q|$ only for small q.

2.5. Renormalization group

The long-wavelength limit of equation (6) has been studied using the RG [11] in connection with several different problems [12, 13]. We shall cite the results here without deriving them.

From the $|q|$ form of the propagator for small q, one can see from power counting that the $u(x)$ field is dimensionless in the absence of loop corrections. This is similar to the Kosterlitz–Thouless transition [14]—or the sine-Gordon model—in 2D systems. Unlike the case there, however, the singular form of the propagator here prevents any renormalization of u (or equivalently of β) to any loop order.

If the potential $V(u)$ is expanded in its harmonics, all higher harmonics die away rapidly compared to the lowest one, and can be neglected. Replacing $V(u)$ with $g\cos(2\pi u/f)$, one obtains a 1D long-range version of the sine-Gordon model. Calculating one-loop corrections, one finds $\mathrm{d}g/\mathrm{d}l = g(1-2/\beta f^2) + \mathrm{O}(g^3)$ (shifting u by $f/2$ shows that there is a $g \to -g$ symmetry) and hence the operator g is irrelevant for $\beta < 2/f^2$, and relevant for $\beta > 2/f^2$. Although this is a weak-coupling result, it has been argued to be true even for large g. At $\beta = 2/f^2$, by mapping the problem to the scattering from a potential of 1D free fermions, it can be shown that the behaviour is not universal, and depends on g.

In the high-temperature phase, equation (6) thus renormalizes to a harmonic phonon energy. The form of the density–density correlations can be obtained from the following argument. The deviation of the density from the mean has a lowest Fourier component of

the form $\delta\rho(x) = \cos(2\pi f x + \theta(x))$, where $\theta(x)$ varies more slowly than the oscillations in $\cos(2\pi f x)$. Comparison with the definition of the (coarse-grained) displacement field $u(x)$ shows that this is effectively $\cos[2\pi(fx+u(x))]$. The connected part of the density correlation function is then of the form

$$K_c(x-y) \sim \langle \delta\rho(x)\delta\rho(y)\rangle \sim \langle \cos 2\pi(fx+u(x)) \cos 2\pi(fy+u(y))\rangle. \quad (13)$$

Using the fact that $u(x)$ is a Gaussian field, this simplifies to

$$K_c(x-y) \sim \cos 2\pi(fx-fy) \exp\{-2\pi^2\langle[u(x)-u(y)]^2\rangle\} \sim \frac{\cos 2\pi(fx-fy)}{|x-y|^{4/\beta}} \quad (14)$$

where the last expression is an asymptotic result. Thus $K_c(x-y)$ is a product of two terms: a rapidly oscillating factor, corresponding to the periodicity of the ideal crystalline state, and a factor that decays as a power of the separation between the points. In the low-temperature phase, where g is relevant, $u(x)$ is almost always at the minima of the potential $V(u)$, and there is LRO in the system. This is easiest to see in the kink representation.

For $\beta > 2/f^2$, proceeding through the kink representation yields equation (6), with $\beta \to 4/(\beta f^4)$, i.e. in the high-temperature phase. As we shall now see, the resulting *irrelevance* of the operator g implies LRO in the kink representation. The relative phase of the local periodic structure at two points x and y, compared with a reference crystalline configuration, is $2\pi f\{n_k(x,y)-n_{\bar{k}}(x,y)\}$, where $n_k(x,y)$ and $n_{\bar{k}}(x,y)$ are the number of kinks and antikinks respectively between x and y. As in the phonon representation, the correlation function is then of the form

$$K_c(x-y) \sim \langle \exp[2\pi \mathrm{i} f\{n_k(x,y) - n_{\bar{k}}(x,y)\}]\rangle. \quad (15)$$

Since in the kink representation the potential $V(u)$ in equation (6) with $\beta \to 4/\beta f^4$ is interpreted as the generating function for the kinks and antikinks, the right-hand side of equation (15) can be obtained by changing $V(u)$ in the region between x and y from $g\cos(2\pi u/f)$ to $g\cos(2\pi f + 2\pi u/f)$ (so that $\mathrm{e}^{\pm 2\pi \mathrm{i} u/f}$ picks up a factor of $\mathrm{e}^{\pm 2\pi \mathrm{i} f}$). If the partition function thus modified is denoted by $Z(g,g')$, and the original partition function by $Z(g,g)$, we have

$$\langle \exp[2\pi \mathrm{i} f\{n_k(x,y) - n_{\bar{k}}(x,y)\}]\rangle = \frac{Z(g,g')}{Z(g,g)}. \quad (16)$$

If g is an irrelevant operator, this flows to a constant at long distances under renormalization (the value of the constant depends on the finite corrections that are removed along the course of the renormalization flow), and there is LRO. By expanding the right-hand side of equation (16) in powers of g for small g, it can be seen that the correlation function decays to its long-distance limit with a power law transient rather than an exponential.

An alternative way to understand the correlations in the kink representation is to start with equation (12). At low temperatures, the system consists of bound pairs of kinks and antikinks. The probability that the number of kinks and antikinks between two points x and y separated by a large distance are not matched, is then dominated by cases when a kink (antikink) lies just inside the interval (x,y) and its partner lies just outside. This is clearly independent of the separation between x and y when the separation is large, so that $K_c(x-y)$ goes to a non-zero limit for large $|x-y|$. The phase transition then corresponds to an unbinding point, where the mean separation between bound pairs diverges, i.e. $\int^{|x-y|} \mathrm{d}l\ (l/l^{\beta f^2})$ diverges for large $|x-y|$. This occurs at $\beta = 2/f^2$. Beyond this point, there is a proliferation of kinks and antikinks; for large separations $\mathrm{mod}(n_k - n_{\bar{k}}, 1/f)$ is equally likely to assume any of its allowed values, and there is no LRO.

In more detail, the density–density correlation function can be expressed in terms of the set of functions

$$C^{(\nu)}(j-k) = \langle \exp\{2\pi \mathrm{i}\nu(u_j - u_k)\}\rangle \tag{17}$$

with $\nu = 1, 2\ldots$. The preceding discussion only deals with $\nu = 1$; other values of ν give rise to corrections to the correlation function that decay more rapidly, and therefore do not affect the leading asymptotic behaviour.

3. Exact duality in Villain–sine-Gordon theory

In this section we consider a particular type of sine-Gordon theory that corresponds to a Villain approximation [15] of the cosine function, hence the Villain–sine-Gordon model (VsG). The advantage of this model is that one has an exact duality reminiscent of the Kramers–Wannier duality in the 2D Ising model. Towards this end we begin by considering a model for the energy in the sense of models described in equation (6), a sine-Gordon model given by

$$\beta H_{sG} = \frac{\pi\beta}{2}\sum_q h_q \tilde{u}_q \tilde{u}_{-q} + \beta g \sum_{j=1,N}[1 - \cos(2\pi u_j/f)]. \tag{18}$$

The Gaussian propagator h_q is specified partly by giving its leading behaviour as $h_q = |q| + \mathrm{O}(q^2)$ for small q, the sum is over the N wavevectors q, obeying $-\pi \leqslant q \leqslant \pi$. The partition function is obtained by writing

$$Z_{sG=} \int \Pi_j \, \mathrm{d}u_j \, \exp(-\beta H_{sG}).$$

The Villain version of this model is defined by the partition function

$$Z_{VsG}[\beta, g] = \sum_{\xi_j=0,\pm1,\ldots} \int \Pi_j \, \mathrm{d}u_j \, \exp\left[-\frac{\pi\beta}{2}\sum_q h_q \tilde{u}_q \tilde{u}_{-q} - \frac{2\pi^2}{f^2} g\beta \sum_j (u_j - f\xi_j)^2\right] \tag{19}$$

corresponding to a periodic function replacing the cosine in equation (18), as usual, with the correct quadratic coefficient. The VsG model is defined by the above partition function, and the rules for computing the correlation functions given in equation (17), in terms of which the original density–density correlation function of equation (2) can be expressed. (Formal expressions for $C^{(1)}(j-k)$ for the VsG model are given in the appendix, but the RG arguments of the previous section are sufficient to obtain the qualitative behaviour.) The evaluation of the partition function is done by two different ways, leading to the same kink partition function, but with different parameters, and hence the duality follows.

The first method. This is similar to the phonon representation described above, and is based on the Poisson summation formula:

$$\sum_{\xi_j=0,\pm1,\ldots} \exp\left[-\frac{2\pi^2}{f^2} g\beta (u_j - f\xi_j)^2\right] = \sqrt{\frac{1}{2\pi g\beta}} \sum_{m_j=0,\pm1,\ldots} \exp\left[\frac{2\pi \mathrm{i} m_j u_j}{f} - \frac{m_j^2}{2g\beta}\right].$$

This is substituted in equation (19), leading to a shifted Gaussian in the variables $\tilde{u}_q$, which can be integrated out, yielding a product form for the partition function

$$Z_{VsG}[\beta, g] = (2\pi g\beta)^{-N/2} Z_{gauss}(\beta, \{h_q\}) Z_{vortex}[\beta, g] \tag{20}$$

with

$$Z_{gauss}(\beta, \{h_q\}) = \Pi_q \left(\frac{2}{\beta h_q}\right)^{1/2}. \tag{21}$$

With $\tilde{m}_q$ defined as $1/\sqrt{N}\sum \exp(\mathrm{i}qj)m_j$, Z_{vortex} is given by

$$Z_{vortex}[\beta, g] = \sum_{m_j=0,\pm1,\ldots} \delta_{0,\sum m_j} \exp\left[\left(-\frac{1}{2\beta g}\right)\sum m_j^2 - \frac{2\pi}{\beta f^2}\sum_q \frac{1}{h_q}\tilde{m}_q\tilde{m}_{-q}\right] \tag{22}$$

where the constraint $\sum m_j = 0$, arises from the vanishing of h_q at small q.

The second method. In equation (19) we fix a set of $\{\xi_j\}$ and then shift the variables $u_j = u'_j + f\xi_j$. Next, we integrate out the (still Gaussian) variables u'_j using

$$\langle \tilde{u}'_q \tilde{u}'_{-q}\rangle = \frac{1}{\beta\pi}\frac{1}{h_q + \alpha^{-1}} \tag{23}$$

where α is defined as

$$\alpha = \frac{f^2}{4\pi g} \tag{24}$$

and find a factorization

$$\begin{aligned} Z_{VsG}[\beta, g] &= Z_{gauss}[\beta, \{h_q + \alpha^{-1}\}]Z_{rough}[\beta, g] \\ Z_{rough}[\beta, g] &= \sum_{\xi_j=0,\pm1,\ldots} \exp\left[-\frac{1}{2}\beta\pi f^2 \sum_q \frac{h_q}{\alpha h_q + 1}\tilde{\xi}_q\tilde{\xi}_{-q}\right]. \end{aligned} \tag{25}$$

The second part of the above is best seen as a roughening model with discrete height variables $\xi_j = 0, \pm1, \ldots$ interacting with a potential that is long-ranged $\sim 1/r^2$, since the propagator is linear in $|q|$, for small $|q|$. In order to proceed, we define dual variables: $\eta_j = \xi_{j+1} - \xi_j$. These satisfy the condition $\sum \eta_j = 0$ due to periodic boundary conditions and have a natural interpretation in terms of height differences in the roughening model. In terms of Fourier components $(\tilde{\eta}_q, \tilde{\xi}_q) = 1/\sqrt{N}\sum \exp(\mathrm{i}qj)(\eta_j, \xi_j)$, we have $\tilde{\eta}_q = (\exp(\mathrm{i}q) - 1)\tilde{\xi}_q$, and so the roughening model becomes

$$Z_{rough}[\beta, g] = \sum_{\xi_j=0,\pm1,\ldots} \exp\left[-\frac{1}{4}\beta\pi f^2 \sum_q \frac{h_q}{(\alpha h_q + 1)(1 - \cos(q))}\tilde{\eta}_q\tilde{\eta}_{-q}\right]. \tag{26}$$

The propagator is now again of the form $\frac{1}{|q|}$ for small $|q|$, and hence we can hope to get a more exact equality. This motivates us to choose the function $h_q \to h_q^*(\alpha)$ which satisfies a quadratic equation:

$$\frac{1}{4}\pi f^2 \frac{h_q^*}{(\alpha h_q^* + 1)(1 - \cos(q))} = \frac{f^4}{4}\left[\frac{2\pi\alpha}{f^2} + \frac{2\pi}{f^2 h_q^*}\right]. \tag{27}$$

Thus, provided $\alpha \leqslant \frac{1}{2}$, we have a self-dual propagator

$$h_q^* = \frac{2|\sin(q/2)|}{1 - 2\alpha|\sin(q/2)|}. \tag{28}$$

It is readily seen that $h_q^* = |q| + \mathrm{O}(q^2)$ for small $|q|$. This choice gives

$$Z_{rough}[\beta, g] = \sum_{\xi_j=0,\pm1,\ldots} \exp\left[-\frac{1}{4}\beta\pi f^4 \sum_q \left(\frac{1}{g} + \frac{2\pi}{f^2\, h_q^*}\right)\tilde{\eta}_q\tilde{\eta}_{-q}\right] \tag{29}$$

$$= Z_{vortex}\left[\frac{4}{\beta f^4}, g\right]. \tag{30}$$

The second equation follows from comparing the first with the definition of the vortex partition function equation (22). For the self-dual propagator, h_q^*, we see that Z_{rough} and Z_{vortex} are in

fact *independent* of g, and are equivalent to the model studied earlier by Kjaer and Hilhorst [9]. However, the original Z_{VsG} is still g dependent. The implications of this will be discussed further in the last section of this paper. Hence we have the final result:

$$Z_{VsG}[\beta, g] = Z_{gauss}[\beta, \{h_q^* + \alpha^{-1}\}] Z_{vortex}\left[\frac{4}{\beta f^4}\right]. \tag{31}$$

A comparison of the above with equation (20) provides the exact duality relation for this choice of h_q^*:

$$Z_{vortex}\left[\frac{4}{\beta f^4}\right] = Z_{vortex}[\beta] \Pi_q \left(\frac{h_q^* + \alpha^{-1}}{2\pi g \beta h_q^*}\right)^{1/2}. \tag{32}$$

There are several comments to be made at this point. First, the restriction $\alpha \leqslant \frac{1}{2}$ implies that the coupling constant g must be large enough in equation (19); too weak a periodic potential would have large fluctuations in $\tilde{u}_q$, that are not acceptable to this relation. In the limit of infinite g the relation is particularly simple, namely $\alpha = 0$ and hence $h_q^* = 2|\sin(\frac{q}{2})|$. In this case the Villain approximation also would be exact for the sine-Gordon model equation (18). The series of equivalences that have been established here can be summarized in the following diagram:

$$\begin{array}{ccc} Z_{VsG}[\beta, g] & \longleftrightarrow & Z_{vortex}[\beta] \\ \Updownarrow & & \uparrow \\ Z_{rough}[\beta] & & Z_{rough}\left[\dfrac{4}{\beta f^4}\right] \\ \downarrow & & \Updownarrow \\ Z_{vortex}\left[\dfrac{4}{\beta f^4}\right] & \longleftrightarrow & Z_{VsG}\left[\dfrac{4}{\beta f^4}, g\right]. \end{array} \tag{33}$$

Here the symbols $\downarrow$, $\Updownarrow$ and $\longleftrightarrow$ symbolize relations via equations (29), (25) and (20), respectively. We see that the critical temperature of the model, if unique, is constrained to be $\beta_c = 2/f^2$. There is of course no guarantee that there is no other critical point, if so, they must occur in pairs and satisfy the product condition $\beta_{1c}\beta_{2c} = (2/f^2)^2$. As mentioned earlier, it has been argued from RG considerations that there is only a single critical point; numerical evidence is presented in the next section.

4. Numerical results

The results in the previous sections have been based on perturbative calculations in the parameter g to obtain its relevance or irrelevance under renormalization. Although it has been argued that such perturbative considerations are in fact valid for all g [11] for the continuum sine-Gordon theory, it is nevertheless useful to compare the results with numerical simulations, since the large g regime could be different for the continuum and discrete models.

Correlation functions for the DCG on a ring were computed numerically. Only the case of half-filling ($f = \frac{1}{2}$) was considered. The numerics were performed by starting in an ordered configuration, and evolving the system under Monte Carlo dynamics for some temperature. Various values of β were chosen, starting from $\beta = 4$ on the high-temperature side, to $\beta = 9$ on the low-temperature side. This range covers the freezing transition at $\beta = 2/f^2 = 8$.

Figure 2 shows a log–log plot of the connected part of the correlation function, $K_c(r)$, as a function of r for $\beta = 4$. For convenience of representation, a factor of $(-1)^r$ has been removed from $K_c(r)$, so that it represents the deviation from perfect crystalline order. Lattice

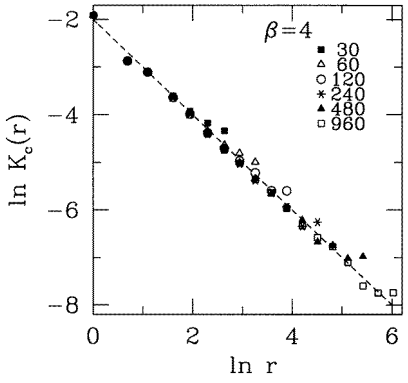

Figure 2. Log–log plot of the correlation function for $\beta = 4$. System sizes range from 30 to 960. Error bars are smaller than the symbols (except for the last three points). The broken line corresponds to a power law with exponent -1, as per the exact result of Mehta [7].

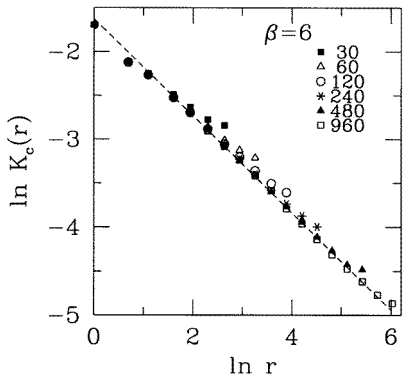

Figure 3. Log–log plot of the correlation function for $\beta = 6$. System sizes range from 30 to 960. Error bars are smaller than the symbols. The broken line corresponds to a power law with the best fit exponent -0.553, which is significantly different from the theoretical result. This can be understood in terms of corrections to the scaling form, as shown in figure 4.

sizes of $L = 30$ through 960 were used. The correlation function is described very well by a power law decay with an exponent 1: $K_c(r) \sim 1/r$. This is in agreement with the exact result [7].

For any $\beta < 8$, we expect a power law decay of $K_c(r)$ with an exponent $4/\beta$. However, figure 3 shows a log–log plot of $K_c(r)$ for $\beta = 6$; the apparent slope is significantly different from $4/\beta = \frac{2}{3}$.

One has to be careful in interpreting this result, since as $\beta \to 8$, the irrelevant operator g renormalizes to zero more and more slowly, so that corrections to scaling could affect the apparent exponent over a fairly wide regime. To test whether the slope in figure 3 can indeed be explained by leading irrelevant corrections, we try to fit the correlation function to the scaling form $K_c(r) \sim r^{-2/3}\hat{K}_c(r/L; gr^{-1/3})$. This is the specific case for $\beta = 6$ of the general scaling form

$$K_c(r) \sim \frac{1}{r^{4/\beta}}\hat{K}_c(r/L; gr^{(1-8/\beta)}) \tag{34}$$

based upon the RG flow of g, namely $\mathrm{d}g/\mathrm{d}l = g(1-8/\beta) + \mathrm{O}(g^3)$, with $K_c(a, b)$ possessing a regular expansion for $a, b \sim 0$. If $K_c(r)r^{2/3}$ is obtained for $r = \lambda L$ for fixed λ and varying L, the result should then be a function of λ and $gr^{-1/3}$. For small g, one would expect this to be a linear function of $r^{-1/3}$. Figure 4 shows such a plot of $K_c(r)r^{2/3}$ as a function of $r^{-1/3}$ for various values of λ. A set of straight lines is obtained, consistent with the scaling prediction.

In view of the strong dependence on β of the dimension of the operator g, it is not very useful to try this for larger values of β, since the range one obtains for $L^{1-8/\beta}$ is quite limited. Conversely, there is no sign of any corrections to scaling for $\beta = 4$, because of the rapid decay of g under renormalization.

At $\beta = 8$, the operator g is marginal. This is not just a perturbative result; based on the continuum model, one expects a line of fixed points for $\beta = 8$, with continuously varying asymptotic behaviour as the initial g is varied. In order to check this scenario, we performed Monte Carlo simulations on a slightly modified version of the DCG at half-filling. The lattice size was doubled, corresponding to $f = \frac{1}{4}$, but the particles were biased to be on the even sites of the lattice by adding an extra potential to the odd sites. It is clear that if the bias is

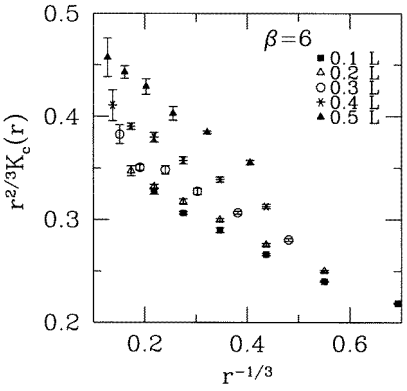

Figure 4. Correlation function for $\beta = 6$, multiplied by its asymptotic power law decay. The x-axis plots the r-dependence of the leading irrelevant operator, g. The different symbols correspond to $r = \lambda L$ with different values of λ. Apart from the smallest values of r, the data fits reasonably well to a set of straight lines. Note that r decreases along the x-axis.

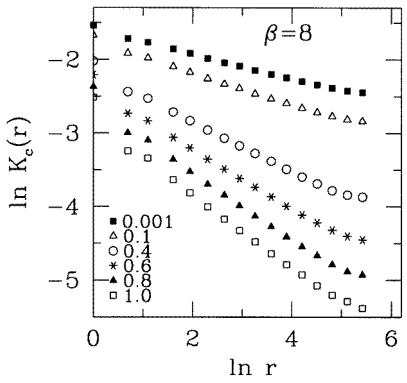

Figure 5. Log–log plot of the correlation function for $\beta = 8$, and system size $L = 960$ showing the effect of varying the initial g, a marginal operator. Error bars are smaller than the symbols. The different curves correspond to different values of the bias, which is the relative 'Boltzmann' weight of the odd sites compared to the even sites. The correlation function is computed by first coarse graining the density, so that there are effectively 480 sites (corresponding to 240 particles at half-filling), and removing the factor of $(-1)^r$. As the bias changes, the correlation function evolves smoothly, with no universality seen even for large r.

infinite, the system is equivalent to the DCG at half-filling, while with zero bias, one has the DCG at quarter filling. In general, the lattice structure can be represented as a strong (strictly speaking, singular) potential $W(u)$ that is periodic under $u \to u + \frac{1}{4}$, and an additional weak potential $V(u)$ that is periodic under $u \to u + \frac{1}{2}$. The strength of $V(u)$ depends on the bias favouring the even sites. Since $W(u)$ is irrelevant for $\beta < 32$, only the potential $V(u)$ affects the asymptotics. As one adjusts the bias, which corresponds to changing g, one should see a continuous evolution in the asymptotic behaviour of $K_c(r)$. Figure 5 shows that this is indeed the case for $L = 960$.

Beyond the transition, figure 6 shows the correlation function for $\beta = 9$, indicating that LRO has set in. The slow decay of the operator g in the dual representation (since $64/\beta$ is not much less than eight) leads to the long transients in the correlation function. By comparison, the correlation function at $\beta = 10$, shown in figure 7, approaches the asymptotic $r \to \infty$ limit much more rapidly. We did not increase β beyond this, because we do not expect to see any qualitative change in the correlation function, and because as β is increased, it takes progressively longer for the system to equilibrate.

Thus we see that the numerical results at half-filling for the density density correlation function agree on both sides of the freezing transition with the analytical results obtained in the previous sections.

5. Discussion

In this paper, we have obtained the phase diagram for the 2D Coulomb gas on a 1D lattice, which emerges as a generalization of the wavefunction of a spin-$\frac{1}{2}$ Heisenberg antiferromagnet in one dimension. We have seen that the gas freezes into a state with LRO below a freezing

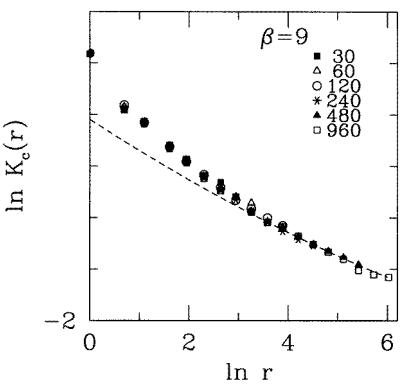

Figure 6. Log–log plot of the correlation function for $\beta = 9$. System sizes range from 30 to 960. Error bars are smaller than the symbols. The broken line is of the form $A + Br^{-1/8}$, which includes the leading scaling correction to the LRO. The parameters A and B are adjusted for approximately the best fit to the eye, and are both equal to 0.1.

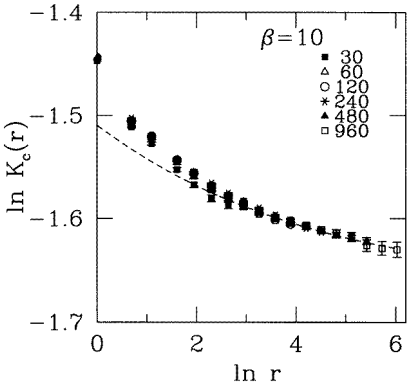

Figure 7. Log–log plot of the correlation function for $\beta = 10$. System sizes range from 30 to 960. The broken line is of the form $A + Br^{-1/4}$, which includes the leading scaling correction to the LRO. The parameters A and B are adjusted for approximately the best fit to the eye, and are chosen to be $A = 0.189$ and $B = 0.032$. With these parameters, $C(\infty)/C(0)$ is estimated to be approximately 0.75.

temperature $T_c = f^2/2$ that decreases as the density is reduced. Above this temperature, the gas has quasi LRO, with continuously varying exponents. The dependence of the LRO on β is thus quite dissimilar to the dependence of LRO upon Δ in the XXZ model. In the latter, the isotropic point is at the brink of crystallization, whereas in this problem, the wavefunction at $\beta = 4$ for the Haldane Shastry model [1,2] is well inside the power law phase, since crystallization only sets in for $\beta > 2/f^2$. On the other hand, the wavefunctions require 'umklapp' for $\beta > 2/f$ beyond which the kinetic energy ceases to act in a simple way on these functions [4].

The strong connections that exist in earlier work [9–12,16] have been alluded to; we return to them here in more detail. In section 3, we considered a one-parameter family of Villain–sine-Gordon models at each temperature, to obtain an exact duality transformation; the family was parametrized by g. Rather surprisingly, all the models in the one parameter family map to the same roughening model, independent of g. As shown in the appendix, formal expressions for the correlation functions of the VsG model can be obtained in terms of the roughening model, with the parameter g affecting the expressions only at short distances. This implies that, for any inverse temperature β, all the VsG models (independent of g) flow to the same fixed point under renormalization. Although this is reasonable at any other temperature, it is somewhat unexpected for $\beta = 2/f^2$, where one has a line of fixed points. Although g is a marginal operator here, the self-dual propagator h_q^*, and therefore the strength of the irrelevant operators, depend on g. One must conclude that, within the one parameter family that we construct, this change in the irrelevant operators is just sufficient to drive g to the same fixed point under renormalization, regardless of its bare value. Of course, one could obtain a duality mapping between VsG models with different, 'conjugate', choices of h_q, chosen to satisfy $2(1 - \cos q)(\alpha + 1/h_q) = h'_q/(1 + \alpha' h'_q)$. However, although this would allow one to access other fixed points at $\beta = 2/f^2$, one would not have (strict) self-duality.

As mentioned earlier, the roughening model constructed in section 3 has been studied earlier by Kjaer and Hilhorst [9]. They obtained the phase diagram we have here, and at (in our notation) $\beta = 2/f^2$, exploit the self-duality to calculate the $\langle m_q m_{-q} \rangle$ correlator. As shown

in the appendix, the correlation function for the VsG model (and ultimately the Coulomb gas) is related to $\langle \exp \mathrm{i}[m(x) - m(y)] \rangle$. It is tempting to conjecture that $m(x)$ can be treated as a Gaussian variable for the long-distance form of this correlation function, especially because using the result of Kjaer and Hilhorst then yields a power law decay for the VsG correlation at the self-dual point with the *same* exponent, $\frac{1}{4}$, with two different approaches given in equations (A2) and (A3). However, numerical simulations we have conducted for the VsG model ($f = \frac{1}{2}, \beta = 8$) do not bear this out: the numerical exponent is approximately $\frac{1}{8}$.

The continuum version of the long-range 1D sine-Gordon has been studied extensively in connection with dissipative quantum mechanics [10], Luttinger liquids [11], and the quantum Hall effect [12]. However, the duality transformation is slightly different from the discrete case [10]. For large g, $u(x)$ must be close to an integer everywhere; a kink consists of a rapid change of $u(x)$ from one integer to another. If (without a lattice cut-off) the theory is regulated with an mq^2 term in the propagator for u, it is clear that $u(x)$ cannot change discontinuously. The competing effects of g and m then yield an effective kink size of $\sim \sqrt{m/g}$, and a kink fugacity of $\sim \exp(-\beta\sqrt{mg})$. This is equivalent to a sine-Gordon theory expanded in powers of the cosine interaction, provided one chooses $g_D \sim \exp(-\beta\sqrt{mg})$. Thus we see that the large g regime maps to small g under duality. This is in contrast to the discrete model, where u_i can jump from one integer to another as i increases by 1, without any extra (i.e. not accounted for by h_q) energy associated with the kink. Indeed, in the Villain version studied in section 3, a large g maps to the same (large) g under duality.

The RG flows for the continuum model were obtained [11] in the small coupling constant regime. Exploiting the duality transformation, it was possible to obtain the RG flows for very large coupling constants as well. It was argued that the RG flows could be connected smoothly between these two extremities; this was strengthened by showing that at the self-dual 'temperature', which corresponds to the scattering of non-interacting fermions from a barrier in the Luttinger liquid version, one should indeed have a line of fixed points.

While for a small coupling constant the discrete and continuum versions should not differ in any physical way, this is not necessary when the coupling constant is large. Thus the possibility of a non-trivial strong coupling phase cannot be ruled out for the discrete model based on continuum arguments. Our numerics indicate that the Coulomb gas shows the same behaviour as the continuum model, suggesting that it is unlikely that there is such a strong coupling phase. Notice that, although the RG flows are oppositely oriented for $\beta > 2/f^2$ and $\beta < 2/f^2$, under the duality transformation of section 3 a larger coupling constant maps to a larger coupling constant, emphasizing the importance of the simultaneous change in the irrelevant operators.

A 1D Coulomb gas with logarithmic interactions was considered earlier by Anderson *et al* [17] in their study of the Kondo problem. This is equivalent to the kinks in a ferromagnetic Ising spin chain with long-range coupling $\sim 1/r^2$. However, the ferromagnetic nature of the underlying order forces charges to alternate. As shown by a real space RG calculation [17], integrating out tightly bound charge pairs renormalizes the strength of the logarithmic interaction between the remaining charges. Thus β flows under the RG, and one obtains the 2D Kosterlitz–Thouless [14] phase diagram. For finite coupling constants (or charge fugacity), this prevents one from exactly obtaining the phase transition point.

Note added in proof. Professor P J Forrester has brought his paper [18] to our attention. This work addresses the effect of adding a periodic potential to the continuous log-gas, and also finds a transition. We thank him for the same.

Acknowledgments

We thank Chandan Dasgupta, Matthew Fisher and Peter Young for useful discussions. BSS thanks the Jawaharlal Nehru Centre for Advanced Scientific Research at Bangalore for partial support; ON is supported in part by the Alfred P Sloan Foundation.

Appendix. Correlation functions

In this appendix, we obtain expressions for the correlation function $C^{(1)}(j)$ within the Villain–sine-Gordon theory using the two methods described in section 3: the low- and the high-temperature limits. We begin by writing the correlation function explicitly as follows:

$$C(k-l;\beta,g) = \langle \exp 2\pi \mathrm{i}(u_k - u_l)\rangle = \frac{1}{Z_{VsG}(\beta,g)} \sum_{\xi_j=0,\pm1,\ldots} \int \Pi_j \, \mathrm{d}u_j \, \exp[\Psi]$$
$$\Psi = -\beta\pi/2 \sum h_q \tilde{u}_q \tilde{u}_{-q} - \frac{2\pi^2}{f^2}\beta g \sum_j (u_j - f\xi_j)^2 + 2\pi\mathrm{i}(u_k - u_l). \tag{A1}$$

We can proceed to evaluate this by the two methods discussed above.

The first method. We use the Poisson formula to trade the integer valued variables ξ_j in favour of the m'_j and find

$$C(k-l;\beta,g) = \frac{1}{Z_{VsG}(\beta,g)} \sum_{\xi_j=0,\pm1,\ldots} \int \Pi_j \, \mathrm{d}u_j \, \exp\Big[-\beta\pi/2 \sum h_q \tilde{u}_q \tilde{u}_{-q} + 2\pi\mathrm{i}/f \sum m'_j u_j \Big]$$

where $m'_j = m_j$ if $j \neq k, l$ and $m'_k = m_k + f$, $m'_l = m_l - f$. Now it is straightforward to integrate out the Gaussian variables u_j and in terms of the variables $\tilde{m}_q$ defined earlier and $\delta\tilde{m}_q = \frac{f}{\sqrt{N}}(\exp(\mathrm{i}qk) - \exp(\mathrm{i}ql))$, we find

$$C(k-l;\beta,g) = \exp\left[-\frac{4\pi}{\beta N} \sum_q \frac{1}{h_q}\{1 - \cos(qk - ql)\} \right] \times \left\langle \exp -\frac{4\pi}{\beta N f^2} \sum_q \frac{1}{h_q} \tilde{m}_q \delta\tilde{m}_{-q} \right\rangle_{vortex[\beta,g]}. \tag{A2}$$

The prefactor decays as a power law at all β, and the average in the second term is over the vortex partition function.

The second method. We fix the variables ξ_j in equation (A1) and shift the variables $u_j = u'_j + f\xi_j$, and integrate over u'_j. We next use the difference variables $\eta_j = \xi_{j+1} - \xi_j$, as in derivation of the roughening model equation (26), and find after some manipulations

$$C(k-l;\beta,g) = \exp\left[-\frac{4\pi}{\beta N} \sum_q \frac{1}{h_q + \alpha^{-1}}\{1 - \cos(qk - ql)\} \right] \times \left\langle \exp \frac{2\pi\,\mathrm{i}}{N} \sum_q \frac{1}{(1+\alpha h_q)(\exp(-\mathrm{i}q) - 1)} \tilde{\eta}_{-q} \delta\tilde{m}_q \right\rangle_{vortex[4/(\beta f^4),g]}. \tag{A3}$$

The remarkable identity of equation (A2) and equation (A3) is a consequence of the two representations of the partition function. These are in general very hard to evaluate, the only simple situation is the case of very low temperatures, where we can assume a dilute gas of vortex–antivortex pairs.

References

[1] Haldane F D M 1988 *Phys. Rev. Lett.* **60** 635
[2] Shastry B S 1988 *Phys. Rev. Lett.* **60** 639
[3] Baxter R J 1982 *Exactly Solved Models in Statistical Mechanics* (New York: Academic)
[4] Shastry B S 1992 *Phys. Rev. Lett.* **69** 164
[5] Mehta M L 1992 *Random Matrices* (New York: Academic)
[6] Gaudin M 1973 *J. Physique* **34** 511
[7] Mehta M L and Mehta G C 1975 *J. Math. Phys.* **16** 1256
[8] Sutherland B 1989 *Interacting Electrons in Reduced Dimensions (NATO ASI Series B Physics vol 213)* ed D Baeriswyl and D K Campbell (New York: Plenum)
[9] Kjaer K H and Hilhorst H J 1982 *J. Stat. Phys.* **28** 621
[10] Schmid A 1983 *Phys. Rev. Lett.* **51** 1506
[11] Kane C L and Fisher M P A 1992 *Phys. Rev. Lett.* **68** 1220
Kane C L and Fisher M P A 1992 *Phys. Rev.* B **46** 15 233
[12] Fisher M P A and Zwerger W 1985 *Phys. Rev.* B **32** 6190
[13] Tsai Y-C 1998 *J. Phys. A: Math. Gen.* **31** 2359
[14] Kosterlitz J M and Thouless D 1973 *J. Phys. C: Solid State Phys.* **7** 1181
[15] Villain J 1975 *J. Physique* **36** 581
[16] Anderson P W and Yuval G 1969 *Phys. Rev. Lett.* **23** 89
[17] Anderson P W, Yuval G and Hamman D R 1970 *Phys. Rev.* B **1** 4464
[18] Forrester P J 1986 *J. Stat. Phys.* **42** 871